**Atmospheric
Chemistry
and Physics
Discussions**

Aerosol formation in
ECHAM5-HAM

R. Makkonen et al.

Title Page

Abstract	Introduction
Conclusions	References
Tables	Figures

◄◄	►►
◄	►
Back	Close

Full Screen / Esc

Printer-friendly Version

Interactive Discussion

Sensitivity of aerosol concentrations and cloud properties to nucleation and secondary organic distribution in ECHAM5-HAM global circulation model

R. Makkonen[1], A. Asmi[1], H. Korhonen[2], H. Kokkola[3], S. Järvenoja[4,†],
P. Räisänen[4], K. E. J. Lehtinen[2,5], A. Laaksonen[2,5], V.-M. Kerminen[4],
H. Järvinen[4], U. Lohmann[6], J. Feichter[3], and M. Kulmala[1]

[1]Department of Physics, University of Helsinki, FI-00014, Helsinki, Finland
[2]Department of Physics, University of Kuopio, FI-70211, Kuopio, Finland
[3]Max Planck Institute for Meteorology, D-20146, Hamburg, Germany
[4]Finnish Meteorological Institute, FI-00101, Helsinki, Finland
[5]Finnish Meteorological Institute, FI-70211, Kuopio, Finland
[6]Institute of Atmospheric and Climate Science, ETH Zurich, CH-8092, Zurich, Switzerland
[†]deceased, October 2007

Correspondence to: R. Makkonen (risto.makkonen@helsinki.fi)

Abstract

The global aerosol-climate model ECHAM5-HAM was modified to improve the representation of new particle formation in the boundary layer. Activation-type nucleation mechanism was introduced to produce observed nucleation rates in lower troposphere. A simple and computationally efficient model for biogenic secondary organic aerosol (BSOA) formation was implemented. We studied the sensitivity of aerosol and cloud droplet number concentrations (CDNC) to these additions. Activation-type nucleation significantly increases aerosol number concentrations in the boundary layer. Increased particle number concentrations have a significant effect also on cloud droplet number concentrations and therefore on cloud properties. We performed calculations with activation nucleation coefficient values of $2\times10^{-7}\,\mathrm{s}^{-1}$, $2\times10^{-6}\,\mathrm{s}^{-1}$ and $2\times10^{-5}\,\mathrm{s}^{-1}$ to evaluate the sensitivity to this parameter. For BSOA we have used yields of 0.025, 0.07 and 0.15 to estimate the amount of monoterpene oxidation products available for condensation. The dynamic SOA scheme induces large regional changes to size distribution of organic carbon, and therefore affects particle optical properties and cloud droplet number concentrations locally. Comparison with satellite observation shows that activation-type nucleation significantly decreases the differences between observed and modeled values of cloud top CDNC.

1 Introduction

Atmospheric aerosols are an important, yet poorly understood, part of the climate system, with largest uncertainties being associated with aerosol-cloud interactions (Lohmann and Feichter, 2005; Penner et al., 2006; Forster et al., 2007; Baker and Peter, 2008). The various effects of aerosols on climate can only be addressed with the help of regional and global climate models. Most current global climate models include the main aerosol types but have a rather simplistic treatment of the aerosol size distribution and associated microphysical processes (e.g. Chen et al., 2007; Jones et

Aerosol formation in ECHAM5-HAM

R. Makkonen et al.

al., 2007; Shindell et al., 2007). This is a serious shortcoming that needs, and probably will, be improved in next-generation climate models (Ghan and Schwartz, 2007; Textor et al., 2007).

The aerosol climate model ECHAM5-HAM (Stier et al., 2005) has a relatively detailed description of aerosol microphysics, making it a promising tool for studying aerosol-climate interactions. However, like practically all other large-scale models, ECHAM5-HAM has a very crude presentation of atmospheric new particle formation and secondary organic aerosol formation. In this study we will investigate how simulated aerosol and cloud droplet number concentrations depend on the implementation of these two processes in ECHAM5-HAM.

Both observations and model studies have shown that atmospheric new particle formation is a significant source of aerosols in the global troposphere (e.g. Kulmala et al., 2004; Spracklen et al., 2006). At present, parameterizations for modeling purposes are available for binary water-sulphuric acid nucleation (e.g. Vehkamäki et al., 2002), ternary water-sulphuric acid-ammonia nucleation (Napari et al., 2002; Merikanto et al., 2007), ion-induced nucleation involving sulphuric acid and water (Modgil et al., 2005), combined ion-induced and neutral formation of sulfate aerosols (Kazil and Lovejoy, 2007), and for so-called "activation-type" and "kinetic-type" nucleation involving sulphuric acid as a driver (Kulmala et al., 2006; Riipinen et al., 2007; Kuang et al., 2008). Most large-scale models include only binary water-sulphuric acid nucleation, which leads to a serious underestimation of new particle formation in continental boundary layers (e.g. Stier et al., 2005; Lucas and Akimoto, 2006). The existing ion-induced nucleation mechanisms seem to suffer from the same problem (Kazil et al., 2006; Lucas and Arimoto, 2006). Ternary water-sulphuric acid-ammonia nucleation appears to perform reasonably well in certain urban centers (e.g. Gaydos et al., 2005), but has a tendency to produce too many particles throughout most of the global troposphere (Lucas and Arimoto, 2006). The activation-type nucleation, while not yet detailed enough to take into account all the influencing factors (e.g. Sihto et al., 2006; Riipinen et al., 2007), appears to be a good candidate for describing boundary-layer nucleation in

global modeling frameworks (Spracklen et al., 2006). Large-scale models cannot usually deal with small clusters formed by nucleation, so it is desirable to combine the used nucleation parameterization with another parameterization able to deal with the initial growth of nucleated clusters to a few nanometers (Kerminen and Kulmala, 2002; Kerminen et al., 2004; McMurry et al., 2005; Lehtinen et al., 2007).

Secondary organic aerosol (SOA) constitutes a substantial fraction of submicron particulate matter in the global troposphere (Tsigaridis et al., 2003; Lack et al., 2004; Fuzzi et al., 2006), in addition to which it plays a central role in coupling atmospheric new particle formation and production of new cloud condensation nuclei (Lihavainen et al., 2003; Kerminen et al., 2005; Laaksonen et al., 2005; Tunved et al., 2006; Spracklen et al., 2008). Most of the atmospheric SOA is believed to originate from biogenic sources, even though also anthropogenic precursor compounds may constitute a significant contribution (Volkamer et al., 2006). Modeling SOA formation in the global atmosphere is subject to large uncertainties (Kanakidou et al., 2005). New schemes to simulate atmospheric SOA formation are being developed continuously (e.g. Griffin et al., 2005; Tulet et al., 2006; Pun and Seigneur, 2007), yet only a few global models are able to simulate SOA formation explicitly (e.g. Chung and Seinfeld, 2002; Tsigaridis et al., 2003; Guillaume et al., 2007; Hoyle et al., 2007; Goto et al., 2008).

In this work, we will run ECHAM5-HAM with both binary water-sulphuric acid and activation-type nucleation schemes. Simulations with and without explicit treatment of SOA formation will be conducted. Our main objectives are to investigate how sensitive simulated aerosol and cloud droplet number concentrations are to the nucleation mechanism, and how important it is to simulate the distribution of SOA over the particle size spectrum explicitly as compared with treating SOA as part of the primary organic aerosol emissions.

2 Methods

2.1 ECHAM5-HAM general circulation model

We use ECHAM5 general circulation model (GCM) with HAM aerosol model (Stier et al., 2005) for global simulations. AEROCOM emissions inventories for year 2000 are used for sulphur compounds, black carbon and organic matter. Emissions of mineral dust, sea salt and oceanic DMS are calculated online. Emissions are treated as primary emissions, except for sulphur compounds, for which 2.5% of emitted mass is considered as primary sulfate emission and 97.5% in the form of sulphur dioxide. The aerosol module HAM includes a chemistry model that treats dimethyl sulfide, sulphur dioxide and sulfate.

HAM uses M7 microphysics to describe aerosol dynamics (Vignati et al., 2005). M7 includes double-moment modal microphysics scheme, where the population is composed of seven log-normal distributions. M7 describes the aerosol distribution with one soluble nucleation mode, and both soluble and insoluble Aitken, accumulation and coarse modes. Standard deviations of the modes are kept constant in our simulations (2.00 for coarse modes, 1.59 for others) and thus advection of only number and mass concentrations is calculated. The upper limits are 5 nm, 50 nm and 0.5 μm for nucleation, Aitken and accumulation mode, respectively. More details on size ranges and dynamics are available in Stier et al. (2005) and Vignati et al. (2005). The most important factor of HAM/M7 regarding this study is the fact that particles have a possibility to grow from one mode to another by condensation, thus a physical connection between nucleation mode (newly formed particles) and larger modes (potential cloud condensation nuclei; CCN) can be made.

We have implemented new nucleation mechanism and dynamic BSOA scheme in M7. Nucleation formulations were done by changing the nucleation subroutines, keeping the dynamics of M7 otherwise as in ECHAM5-HAM. For the BSOA condensation experiment, three new tracers were introduced to include organic matter in soluble nucleation and insoluble accumulation and coarse modes. These modifications had only

Title Page

Abstract | Introduction

Conclusions | References

Tables | Figures

◄ | ►

◄ | ►

Back | Close

Full Screen / Esc

Printer-friendly Version

Interactive Discussion

a minor effect on model computational efficiency.

All Experiments were conducted with T42 horizontal resolution, which corresponds to approximately 2.8°×2.8° grid. Vertically, 19 hybrid levels were used, extending up to 10 hPa. A time step of 30 min was used for all calculations including chemistry and aerosol microphysics. For each simulation, we performed a model spin-up for six months to initialize aerosol fields, and continued with a one-year simulation for analysis. To estimate inter-annual variations, some Experiments were simulated for a five-year period. Resulting statistics are calculated from model output resolution of six hours.

2.2 Cloud droplet activation scheme

We coupled aerosol concentrations to CDNC using the double-moment cloud microphysics scheme by Lohmann et al. (2007), where aerosols are activated as cloud droplets according to Lin and Leaitch (1997) with a $0.035\,\mu$m cut-off radius. Aerosol composition was not taken into account in the activation parameterization. This scheme was used in all simulations throughout this paper. We did not investigate any potential impact on ice clouds.

2.3 New particle formation due to nucleation in atmosphere

Modeling new particle formation is not an easy process to consider in a modal model. Freshly nucleated particles can have sub-nanometer sizes. These particles grow by condensation, but still remain inside the nucleation mode until they reach a radius of ~5 nm. A single lognormal distribution can not keep track of aged nucleation mode particles and freshly formed particles, therefore information of the early growth of particles is lost. In this study, we use a formulation by Kerminen et al. (2004) to estimate the formation rate of particles of 3 nm in size. This was done using the equation (Kerminen and Kulmala, 2002; Kerminen et al., 2004):

$$J_{3\,\mathrm{nm}} = J_{\mathrm{nuc}} \times \exp\left[\gamma \times \left(\frac{1}{3.0\,\mathrm{nm}} - \frac{1}{d_{\mathrm{nuc}}}\right) \times \frac{CS'}{GR}\right], \tag{1}$$

Printer-friendly Version

Interactive Discussion

where J_{nuc} is the nucleation rate of particles of size d_{nuc}, $J_{3\,nm}$ is the formation rate of 3 nm size particles, CS' is proportional to the condensation sink and γ is a function of ambient conditions, properties of the nuclei and pre-existing particle population. Two assumptions were made in calculating the growth rate of sub-3-nm particles (GR) in

5 Eq. 1. First, only sulphuric acid was assumed to condense on particles smaller than 3 nm, and second, the condensational flux of sulphuric acid can be described with the free molecular regime formulation. With these assumptions, we obtain (Kerminen and Kulmala, 2002):

$$GR \approx \frac{3.0 \times 10^{-9}}{\rho_{nuc}} \sum_i \bar{c}_i M_i C_i, \tag{2}$$

10 where GR is in nm hour^{-1}, ρ_{nuc} (kg m^{-3}) is the density of the nuclei, $\bar{c}_i$ (m s^{-1}) is the molecular speed of sulphuric acid, M_i (g mol^{-1}) is its molecular weight and C_i (cm^{-3}) is its vapor concentration. The term 3.0×10^{-9} contains all the constants and conversion factors between the units. Our assumptions may lead to an underestimation of the value of GR below 3 nm. As a result, for a given nucleation rate (J_{nuc}) and size (d_{nuc}),

15 a conservative estimate of $J_{3\,nm}$ will be obtained.

In activation-type nucleation, sulphuric acid "activates" pre-existing clusters for further growth. For this type of nucleation, the actual nucleation rate J_{nuc} can be postulated simply as (Kulmala et al., 2006)

$$J_{nuc} = A \times [H_2SO_4] \tag{3}$$

20 The activation coefficient A contains information about the concentration of the background clusters and dynamics between them and sulphuric acid molecules. The coefficient A varies from one location to another, and for example in Hyytiälä conditions it is reported to be on the order of 10^{-6} s^{-1} (Sihto et al., 2006; Riipinen et al., 2007). Few measurements are available that can provide information about the spatial distri-

25 bution of the activation coefficient, so we have to assume a constant coefficient A for the whole atmosphere. In this study, we assumed a value of 2×10^{-6} s^{-1}, but we tested

the sensitivity of aerosol and cloud droplet concentrations to this coefficient. We also assumed that the radius d_{nuc} of activated clusters is 1 nm.

Binary nucleation in the ECHAM5-HAM is based on Vehkamäki et al. (2002) parameterization of homogenous water-sulphuric acid nucleation. We performed simulations with different implementations of combining the two nucleation methods:

1. activation-type nucleation as a simultaneous process with binary nucleation, where both nucleation mechanism used the same sulphuric acid concentration to estimate $J_{3\,nm}$, and these formation rates were summed up to obtain the apparent formation rate;

2. as above, but with activation nucleation considered only below altitudes of 800 hPa;

3. as 1., but using only the higher $J_{3\,nm}$ of the two methods to calculate the apparent formation rate;

4. assuming that activation nucleation happens first, then recalculating remaining sulphuric acid concentration and then calculation of binary nucleation and;

5. using binary nucleation only, without using Eq. 1.

Most of the Experiments were done using 1. and 5., but we evaluated the sensitivity of the model to the choice of the implementation.

2.4 BSOA distribution mechanism

In the original ECHAM5-HAM SOA formulation, the biogenic monoterpene emissions of Guenther et al. (1995) are used to calculate the formation of biogenic secondary organic aerosol (BSOA). A yield of 0.15 estimates the fraction of oxidation products available for condensation. Oxidation products are handled as primary emissions: the soluble fraction (assumed 65%) is emitted evenly into the soluble Aitken and accumulation modes, and insoluble fraction is emitted into the insoluble Aitken mode. All the

organic mass emitted to insoluble Aitken mode was assumed to be primary particles of size 30 nm. Organic mass emitted to soluble modes is assumed to condense on pre-existing particles.

The dynamic BSOA scheme introduced here does not use any prescribed assumptions about the size distribution or solubility of the organic material. Instead, we use information about the available aerosol surface area. For every grid point in the lowest simulation level, the condensation sink for each mode is calculated from the M7 parameters. This information is then used to estimate the fraction of organic matter condensing on each mode. With M7 we are able to retrieve size distribution of SOA, while bulk aerosol models have to assume a radius for SOA (Goto et al., 2008). Oxidation of emitted biogenic organic compounds, as well as the condensation of oxidation products, is assumed to be so rapid that we can partition the organic vapor directly to the aerosol phase during one time step (30 min) at the point of emission and thus there is no need to transport the organic material. In case of condensation this is a reasonable assumption, except at locations having a very low pre-existing aerosol surface area. The production of condensable vapours by oxidation processes may, however, proceed substantially longer. On the other hand, without knowing the exact oxidation chain of the emitted precursor compounds, assuming an immediate oxidation can be considered as good assumption as any other over which this oxidation might take place. The hygroscopic properties of organic aerosols are treated as in ECHAM5-HAM. The dynamic formulation of BSOA formation allows biogenic organic vapors to condense on freshly formed particles, which increases particle growth rates and hence increases CCN concentrations after new-particle formation events.

3 Results

The Experiments done in this study are listed in Table 1. Experiment B serves as a base-case, since it uses standard ECHAM5-HAM binary nucleation and BSOA scheme. In Experiments A0, A1 and A2 only the nucleation mechanism is modified and

in Experiments S0, S1 and S2 only the BSOA scheme is changed. Experiments AS1 and AS2 describe new particle formation with both activation nucleation and dynamic BSOA scheme.

3.1 Sensitivity of aerosol number distributions and particle formation rates to the choice of nucleation mechanism

Nucleation mode aerosols originate solely from atmospheric new-particle formation in ECHAM-HAM. As a result, the number concentration of nucleation mode particles provides a good measure of the effect of nucleation on particle number concentration without ignoring their coagulation losses below detectable sizes. The number concentration of nucleation mode particles is not directly related to the nucleation rate but it provides a comparable measure for evaluating model results against aerosol measurements. Another factor of interest is the Aitken mode particle number concentration, as it is also somewhat controlled by growing nucleation mode particles and has the potential to have climate effects e.g. by acting as cloud condensation nuclei.

Figure 1 shows the annual average vertical profiles of nucleation mode number concentration and total number concentration without nucleation mode in Experiments B, A0, A1 and A2. Pure binary nucleation produces high nucleation mode number concentrations in the upper troposphere and lower stratosphere with a peak concentration around 200 hPa, which is the only region where binary nucleation rates in average exceed activation nucleation rates. However, concentrations of both nucleation and other modes are low in the boundary layer. Experiments with both binary and activation-type nucleation flatten the vertical profile by increasing concentrations in the lower troposphere and by reducing the binary nucleation peak in the upper troposphere. Part of the difference between B and A simulations in Fig. 1 comes from the fact that Experiments with activation-type nucleation use Eq. 1 to scale nucleation rate to $J_{3\,nm}$. Thus, the average radius of nucleation mode particles in upper troposphere is smaller in Experiment B than in other experiments. This can be seen indirectly in Fig. 1 when comparing concentration of nucleation mode particles to concentration of particles in

Title Page

Abstract	Introduction
Conclusions	References
Tables	Figures

◄ | ►|

◄ | ►

Back | Close

Full Screen / Esc

Printer-friendly Version

Interactive Discussion

larger modes. In the upper troposphere, nucleation mode concentrations produced only with binary nucleation are much larger than concentrations of larger particles, since only a fraction of nucleation mode particles grow to larger sizes. The difference between the concentrations is smaller in activation-type experiments, since average nucleation mode radius is already closer to Aitken mode radius. By taking this into account, solid lines in Fig. 1 are more comparable with each other, since they exclude nucleation mode concentration. It can be seen that even the smallest activation coefficient (Experiment A0) increases the total number concentrations by a factor of 2.5 at the surface.

In Fig. 2, aerosol number concentrations in different size classes are compared between binary nucleation and activation-type nucleation. Figure 2a shows that binary nucleation produces large number concentrations in regions where the temperature and pre-existing aerosol surface area are low and the relative humidity is high. This leads to a band of particles between 100 hPa and 300 hPa with increased concentrations also in lower tropospheric polar areas. In general, concentrations in the lower troposphere are low with only a small increase near 30° N. This lack of particles in the lower atmosphere at mid latitudes is mainly caused by low binary nucleation rates.

A feature of the original ECHAM5-HAM binary nucleation scheme was the absence of Aitken and accumulation mode particles in the upper troposphere at the equator, between 100–200 hPa, which was visible even in annual average concentrations shown in Stier et al. (2005). This behavior is partly due to a minor technical error in application of the Vehkamäki et al. (2001) parameterization in this region: the ECHAM5-HAM formulation sets the nucleation rate to zero outside the validity range of the parameterization. However, even when the values at the limit of the validity range are used when the arguments are outside of the validity range, the tropopause concentrations of nucleation mode particles are less in the tropics than in middle latitudes, even though the difference is much smaller than in figure 4a of Stier et al. (2005).

Results from Experiment A1 (middle panel in Fig. 2) show a similar, but weaker concentration band in the upper troposphere and increased concentrations below 700 hPa,

as compared with Experiment B. The ratio of concentrations (rightmost panel in Fig. 2a) shows that activation-type nucleation increases surface-layer concentrations of nucleation mode particles between 40° S–50° N by an order of magnitude, and concentrations at around 30° N are even 100 times higher than those with the binary nucleation scheme only, mostly due to large sulphur emissions. In the upper troposphere, activation-type nucleation decreases nucleation mode particle concentrations significantly. However, this effect stems mainly from the fact that the average radii of nucleation mode particles produced by binary nucleation (Experiment B) are significantly (2–3 times) smaller than those observed in Experiment A1. Again, number concentrations of particles in larger modes are more comparable with each other.

The results for Aitken and accumulation mode (Fig. 2b and c) are interesting for climate considerations, since nucleation mode particles themselves are too small to be activated into cloud droplets or to interact with atmospheric radiation. Activation-type nucleation increases Aitken mode number concentrations by a factor of 2–3 throughout the surface layer with a high increase near 30° N. In contrast to the nucleation mode, Aitken mode particle number concentrations are increased throughout the atmosphere, with an order of magnitude increase at 100 hPa. This also demonstrates that nucleation mode particles are effectively growing into the Aitken mode. The growth continues until accumulation mode sizes, as can be seen from the increased concentrations of Fig. 2c. While the spatial patterns of nucleation mode and Aitken mode concentrations are significantly altered, the spatial distribution of accumulation mode particles is quite similar in Experiments B and A1: concentrations in the boundary layer are somewhat increased and upper troposphere concentrations show a small decrease. This is due to that majority of accumulation mode particles are from primary emissions. The effect on coarse mode particles was insignificant; changes are purely due to indirect changes in atmospheric dynamics, especially loss processes for largest aerosol particles (e.g. precipitation).

3.2 Sensitivity to the value of activation coefficient

Since the activation coefficient A in Eq. 4 was originally derived from experimental data with limited geographical scale (mostly from boreal forest), it is necessary to investigate how sensitive the aerosol concentrations are to the chosen value of this coefficient. As all the physical and chemical factors affecting the coefficient are currently not known, we have used a constant value for all atmospheric conditions. This choice enables us to estimate the sensitivity of the aerosol concentrations and CDNC to this parameter and to make first estimates of the realistic range of this parameter for further studies.

Figure 3 shows the annual arithmetic-average formation rate of 3 nm particles with activation-type nucleation, and Fig. 4 shows the resulting annual-average nucleation mode particle number concentration in the surface layer for different values of the activation parameter. As expected, the sensitivity of the particle number concentration to the value of A is much lower than the sensitivity of the particle formation rate. The spatial distribution of the total number concentration over the continents does not change dramatically between Experiments A0, A1 and A2. The largest differences can be found in maritime regions, both in continental outflow and over remote ocean areas. Interestingly, results show very little nucleation in tropical rainforest regions of South America, which is in agreement with observations (Rissler et al., 2006).

3.3 Distribution of BSOA over the particle population

In the following, we investigate how the treatment of BSOA formation affects the simulated aerosol properties. Although the modified mechanism we use is rather simple, it is important to know how much the physical representation of the condensation will affect the partitioning of organic species in the aerosol distribution, and how much this affects particle growth and eventually CDNC.

The original ECHAM5-HAM uses constant size and solubility distribution for BSOA emissions. Figure 5 shows how the dynamic SOA model partitions biogenic organic mass between the soluble Aitken and accumulation modes. The original ECHAM5-

HAM assumes a 1:1 partitioning between these modes. On the average, this assumption is rather good in northern hemispheric remote areas, but for many important BSOA source regions organics are condensing mostly on larger particles. In equatorial areas in both Africa and South America the accumulation mode can even be a ten times more efficient sink for BSOA than the Aitken mode. So actually the dynamic BSOA scheme has two counteracting effects regarding CDNC. It allows the condensation of organics onto the nucleation mode and hence provides additional growth for freshly-formed aerosols, which increases Aitken mode particle concentrations and thereby CDNC. However, with the dynamic scheme, more organic mass is partitioned to the accumulation mode compared with the Aitken mode, which on the average decreases CDNC when compared to the original scheme. Figure 5 shows that over boreal forest areas, the Aitken mode is a significant sink for BSOA and hence the dynamic BSOA scheme would increase CDNC.

The dynamic BSOA scheme does not make any assumption about the solubility of the condensing organics; all seven modes are equally likely to act as condensational sinks for the organics. The original ECHAM5-HAM assumes that 65% of the biogenic organic vapors are soluble. Figure 6 shows how different the situation is with the dynamic model. It can be seen that the majority of the organic mass is condensing onto the soluble modes. Condensation onto the insoluble modes reaches a maximum of ∼30% in areas where significant concentrations of insoluble aerosols are available.

3.4 Effects of nucleation mechanisms and BSOA formation to aerosol number concentrations at the surface

Table 2 compares annual median predicted aerosol number concentrations to measured values at several remote locations. Concentrations are provided as CN10 (particle diameter >10 nm) and CN100 (>100 nm). We consider CN10 as a representative of the particle number concentration outside the immediate range of nucleation and CN100 as a rough estimate of CCN. These choices were made for easy comparison with measurements. Activation-type nucleation increases CN10 by a factor of 2 in

several locations (Experiment A1 compared to B). The dynamic BSOA scheme can decrease CN10 in locations of low emissions fields of biogenic organic vapors (Zeppelin and Mace Head), but generally it increases CN10 by a few tens of percent compared to the primary emission scheme. The effect of BSOA on CN100 is not as clear, but the use of dynamic BSOA scheme seems to decrease CN100 (Experiment AS2 compared to A1). In general, the B simulations give better agreement with measurements for CN10 than A simulations in remote areas. On the other hand, modeled concentrations in polluted areas are improved significantly in Experiments with activation nucleation.

3.5 Effects of nucleation mechanisms and BSOA formation to cloud properties

Both activation-type nucleation and dynamic BSOA scheme have significant effects on cloud droplet number concentrations. Since the cloud droplet activation model we use does not take aerosol composition into account, changes in CDNC are only due to changes in the aerosol size distribution. Figure 7 shows how the combined effect of activation-type and dynamic BSOA scheme (Experiment AS1) changes CDNC as compared with CDNC predicted by the original model. The figure shows a histogram of CDNC calculated from annual average CDNC field for the whole atmosphere. Compared with the original ECHAM5-HAM, Experiment AS2 (with both activation nucleation and dynamic BSOA formation) has slightly fewer model grid boxes with CDNC $<25\,\mathrm{cm}^{-3}$. More interestingly, the number of grid boxes with $25\,\mathrm{cm}^{-3}<\mathrm{CDNC}<100\,\mathrm{cm}^{-3}$ is increased significantly. Experiment B has practically no model grid boxes with CDNC above $50\,\mathrm{cm}^{-3}$, but Experiment AS2 has a small but significant number of grid boxes with high CDNC.

The qualitative effect on the CDNC distribution can be seen in Fig. 8, where CDNC in Experiments B and AS2 is presented as a function of latitude and altitude. Similar spatial patterns can be seen in both experiments, which is due to similar annual-average cloud fields generated by ECHAM5-HAM, suggesting that activation-type nucleation did not have significant impact on general cloudiness in these short simulations. CDNC in the Northern Hemisphere reaches its maximum values at 30° N–60° N. The weaker

maximum in the Southern Hemisphere originates from marine emissions and is located more towards the pole, at ∼75° S. Between 30° N–60° N, below 950-hPa level, CDNC is increased at maximum by 60 cm^{-3} due to activation-type nucleation. This kind of an increase might have a significant impact on radiative properties of clouds even in a global scale.

The sensitivity of CDNC against activation coefficient A is presented in Fig. 9, which shows the annual zonal average CDNC in Experiments A0, A1 and A2. It seems that CDNC is rather sensitive to activation coefficient, mainly in the Northern Hemisphere. Differences between Experiments A2 and A1 in 30° N–60° N in BL are in the order of 10–30 cm^{-3}. Still, it must be noted that even Experiment A0 produces significantly increased concentrations when compared with Experiment B. The inclusion of activation-type nucleation and dynamic BSOA scheme increases CDNC significantly in all cloudy areas, and most of this increase is due to nucleation.

Vertical profiles in Fig. 10 provide a more general picture of CDNC in different experiments. Figure 10 shows that over land, all Experiments with activation-type nucleation increase CDNC by a factor of 2 throughout the atmosphere, and that the effect is slightly stronger above oceans. Also the sensitivity to the activation coefficient is stronger in maritime atmosphere. This higher sensitivity to nucleation method is due to relatively higher proportion of CDNC in remote oceans from nucleation as the primary particle numbers and hence coagulation sinks in these areas are much lower. It can be seen that on average, the use of the dynamic BSOA scheme decreases CDNC (solid blue and green lines) and an increase in BSOA yield will decrease CDNC. Since our model considers only continental BSOA sources, the BSOA scheme has practically no effect over oceans.

Figure 11 presents cloud-top CDNC over maritime regions in Experiments B and AS2. Primary emissions and binary nucleation in Experiment B produce very low cloud-top concentrations. Only a few small areas have CDNC above 100 cm^{-3}, and most values are around 60 cm^{-3}. Highest concentrations are situated in two belts, between 10° N and 50° N in the Northern Hemisphere and between 0° S and 50° S in

the Southern Hemisphere. As with zonal patterns, activation-type nucleation does not change the spatial distribution of CDNC but increases cloud-top CDNC in areas with high sulphuric acid concentration. Maximum average values reach 400 cm^{-3} in Experiment AS2. There is some increase in all ocean basins, mainly near the coasts. Major
5   differences are found, however, in regions of a continental outflow: west of North- and South-America, Europe and South-Africa, and east of China due to higher nucleation rates over the continents. Parts of these areas are defined in Fig. 11 and examined in detail in Table 3. Binary nucleation significantly underestimates cloud top CDNC in all regions considered. Experiments A0, A1 and A2 increase cloud top CDNC in average
10 by factor of 2.1, 3.1 and 3.8 in comparison with Experiment B, respectively. Activation nucleation in general gives much better agreement with measured values, especially Experiment A0.

3.6   Temporal variability of aerosol and cloud droplet number concentrations

Since our simulations do not use nudging of meteorological fields, we have to quantify
15 the error caused by different meteorology in the experiments. In order to estimate the inter-annual variability of aerosol and cloud droplet concentrations, we extended Experiment AS2 over a five-year simulation period. In case of the vertical profiles of aerosol concentrations (Fig. 1), the standard deviation for five distinct years is less than 1% of the corresponding annual average particle number concentrations. CDNC are more
20 sensitive to changes in model meteorology than aerosol concentrations. The standard deviation of annual global average CDNC above land (Fig. 10a) reaches a maximum of 4 cm^{-3} at 1000 hPa and stays below 1 cm^{-3} above the 800-hPa altitude. The difference in CDNC above land between Experiments AS2 and B is therefore 15 times larger than the inter-annual standard deviation. Above oceans (Fig. 10b), the standard deviation
25 is lower (maximum 1.6 cm^{-3}) and the signal due to activation-type nucleation is about 30 times larger than the standard deviation. It should be noted that global averaging reduces the effect of inter-annual variability: the standard deviation of cloud-top CDNC in regions of Fig. 11 is about 15% of the difference between Experiments AS2 and B.

The intra-annual variability shows also a clear seasonal pattern. With activation-type nucleation, northern-hemispheric aerosol concentrations are highest during the local summer (June and July). Concentrations in the Southern Hemisphere are generally lower, but as with the Northern Hemisphere, they have a peak during the local summer months (December to January).

4 Discussion

Our intention was to present the sensitivity of aerosol and cloud droplet number concentrations to changes in the ECHAM5-HAM nucleation module and BSOA mechanism. By varying related parameters, such as activation coefficient or BSOA yield, we were able to determine the sensitivity of the aerosol and cloud systems.

Comparison of nucleation mechanisms showed a significant sensitivity to the used nucleation mechanism (binary or activation-type nucleation) and a slightly smaller sensitivity to the chosen activation coefficient. However, the use of a constant activation coefficient for the whole atmosphere requires some discussion. Experiments done in this paper show that activation-type nucleation lowers the particle formation rates in upper troposphere in comparison to binary nucleation. This result somewhat decreases the agreement shown in figure 5 of Stier et al. (2005) with aircraft observations. The activation coefficient is a semi-empirical factor based on limited number of surface measurements (Kulmala et al., 2006). In contrast to the binary nucleation scheme used, which is based on solid thermodynamic basis, the activation-type nucleation process itself is not well known. For example, the exact relationships between the coefficient A and other physical parameters are poorly known. Likewise, there are several indications that the nucleation mechanism in the boundary layer is of either activation or kinetic type (e.g. Sihto et al., 2006; Riipinen et al., 2007; Kulmala et al., 2007; Kuang et al., 2008), it is still somewhat unclear whether activation nucleation is a realistic representation of new-particle formation in the global atmosphere. For these reasons, we can only study the sensitivity of other variables, such as aerosol and cloud droplet num-

ber concentrations, against this coefficient. The coefficient A is a surrogate for possibly many physical and chemical processes behind nucleation, and even though it seems to produce the observed particle formation events quite well near surface in many cases, the use of the same value in the upper atmosphere results in speculative results. The mechanism behind activation nucleation implicitly assumes that sulphuric acid forms stable particles with some other species (e.g. ions, other sulphur chemistry products or organics). However, a constant activation coefficient does imply that the concentrations of these "seeds" are constant in the atmosphere or at least that some competing process compensates changes in pre-existing clusters, which are most probably very rough approximations. On the other hand, recent observations support the idea that the concentration of atmospheric clusters near surface is relatively constant (Kulmala et al., 2007). If we could have more detailed information on the real chemical and physical nature of the activation nucleation, we could scale the coefficient better in upper atmosphere conditions. This formulation would then naturally increase the competing binary nucleation rates drastically, reducing the concentration reduction in the upper atmosphere.

In the binary nucleation case, nucleation and primary emissions together are unable to create realistic aerosol number concentrations in the lower troposphere using the ECHAM-HAM model, as discussed by Stier et al. (2005). The activation nucleation gives, however, very promising results near the surface, creating quite realistic number concentrations of especially Aitken and accumulation modes, which are as yearly averages well comparable with average concentrations from continuous surface measurements. Comparisons in Table 2 show that, in general, Experiments with activation-type nucleation typically give a better agreement in polluted regions but overestimate CN10 in remote areas. We attribute these overestimations partly to high average concentrations with high variability of apparent nucleation rates, which in turn is very closely connected with Eq. 1. Especially the exponent term is sensitive to condensation sink (background aerosol concentration). In reality, it takes longer than one time step (30 min) for newly nucleated aerosol particles to grow to detectable sizes. However, the parameter-

ization of Kerminen and Kulmala (2002) uses only instantaneous aerosol distribution to calculate the removal prior to growth to detectable sizes and adds the surviving newly nucleated particles directly to the model grid box in the same time step. This approach is much more sensitive to local variations in the aerosol concentrations and sulphuric acid concentrations than a more detailed simulation on the smaller particles. However, the method of Kerminen and Kulmala (2002) is better suited for larger scale models: It does not increase the number of tracers, which improves the calculation efficiency, and it does include the main physical processes of growth and losses. Even with the current parameterization, the geometric means of the nucleation mode concentrations and nucleation rates are close to the observed values. This result together with realistic values of Aitken mode number concentrations gives some confidence in using this parameterization to obtain the effective nucleation source rate to the aerosol population near the surface. When comparing the results with Experiment using the original binary nucleation, we must consider the poor performance of modal model representation of nucleation mode in case of strong simultaneous nucleation and growth: fixed standard deviation of nucleation mode distorts the particle number and size in comparison with more realistic size description. Also, all of the comparisons with measurements should be considered as qualitative, as all of the ECHAM5-HAM simulations in this paper were done with model's own (non-nudged) meteorology. Use of a chemical transport model or nudging ECHAM5-HAM would make it easier to compare with field observations, but this study was designed as a sensitivity analysis including all feedback mechanisms of a GCM.

Cloud droplet number concentration was shown to be sensitive to new-particle formation. Firstly, the implementation of activation-type nucleation increased aerosol number concentrations in the lower troposphere and hence provided more seeds for cloud droplets. Secondly, the new dynamic BSOA scheme provided additional growth of freshly formed particles. The cloud droplet activation scheme used in this study had an activation diameter in the Aitken mode of the model, and therefore changes in the Aitken mode led directly to changes in CDNC. If a GCM framework does not include

the possibility of cloud activation in the Aitken mode (as it seems to be the case in many modal models), the resulting CCN numbers might be severely underestimated. Part of the sensitivity estimate does, however, come from the chosen cloud-activation scheme.

Satellite observations provide information on the global scale for multi-year timescales. Unfortunately, instruments used in satellite observations are not able to give direct information about the aerosol size distribution or CDNC, but with several assumptions it is possible to use their estimates for comparison. Bennartz et al. (2007) used two and half years of MODIS satellite data (from July 2004 to December 2005) to produce an overview of CDNC over oceans. Figure 11 shows modeled cloud top CDNC values using the same color scale as in figure 7 of Bennartz et al. (2007). Comparing the Bennartz et al. (2007) Fig. 7 top left subfigure ("all cases") to our Experiment AS2 results show reasonably good agreement on the cloud top CDNC. Since the inter-annual variability of cloud-top CDNC was small, the good agreement is also visible in longer five-year simulations. While binary nucleation is unable to produce observed CDNC near coastlines, activation-type nucleation gives similar results as observed. A good agreement is seen in all five marked regions, as well as in Gulf of Mexico, East of North America and Arabian Sea. From Table 3 one can see that activation-type nucle-ation itself does reduce the differences between modeled and observed CDNC signif-icantly and quantitatively. Experiment A0 performs best in almost all selected regions, but note that it is possible to use other combinations of different activation coefficients and SOA yields outside of the range of values used in these simulations. Also, errata for Bennartz et al. (2007) (Bennartz and Harshvardhan, 2007) discussed the possibility of underestimating the CDNC values on the order of 10% in the presence of aerosols over clouds, which could indicate that simulations A1 or AS1 are closer to observed values. Note that the reported average CDNC values by Bennartz et al. (2007) do not exceed $200\,\text{cm}^{-3}$ although higher values are frequently obtained in both simulations and atmospheric observations (e.g. Miles et al., 2000).

We calculated the nucleation rates using standard ECHAM5-HAM T42 grid. If the

Aerosol formation in ECHAM5-HAM

R. Makkonen et al.

sources or concentrations of the trace gases or aerosols are very non-homogenous, changing the grid size of global-scale simulations can lead to significant changes in the results. We tried to approach this problem by using simulations of different resolutions within ECHAM5-HAM. The results showed that resulting aerosol or cloud droplet number concentrations do not change significantly with changing resolutions. However, part of this result might be due insufficient knowledge of the spatial non-homogeneity of sources and possibly due to the simplified linear nucleation method. It could be that nucleation mechanisms having a non-linear dependence on the sulphuric acid concentration might be more sensitive to resolution changes. Local nucleation rates might be heavily influenced by subgrid-scale changes in the coagulation sink. In many cases, e.g. biomass burning and direct anthropogenic emissions, sulphur dioxide and particle emissions are emitted simultaneously, which could affect nucleation rates in subgrid scales. An addition of a sub-grid emission scheme might be useful in these cases, but for global climate simulations details to that level must be carefully considered.

5 Conclusions

The simulations performed in this study show clearly that aerosol particle number concentrations and, perhaps more importantly, cloud droplet number concentrations in the ECHAM5-HAM model are sensitive to the aerosol nucleation method used. Especially in the boundary layer and upper troposphere, aerosol number concentrations differ greatly depending on the choice of the nucleation mechanism. This sensitivity creates an additional problem for the global climate and earth system models to tackle the problem of realistic aerosol forcing. By using activation-type nucleation and dynamic BSOA method, we get a more realistic description of boundary-layer particle formation events: sulphuric acid activates some background species or ion forming clusters, which grows to 3 nm with sulphuric acid condensation and after 3 nm with the help of biogenic organic vapors. This complete set of processes could allow to better couple vegetation changes and changes in BVOC emissions due to climate change as a

feedback back to the aerosols and climate.

The comparisons to the observations show that activation nucleation is a very promising way to improve the ECHAM5-HAM model closer towards the average values observed over different locations, although the results show high temporal variability with occasionally unrealistically high number concentrations in polluted areas CDNC comparisons to the satellite data show that even with the large uncertainties associated with both nucleation and cloud activation, the direction of the changes is clearly towards a better representation of aerosol number and cloud droplets number concentration in the atmosphere.

References

Aalto, P., Hämeri, K., Becker, E., Weber, R., Salm, R., Mäkelä, J. M., Hoell, C., O'Dowd, C. D., Karlsson, H., Hansson, H.-C., Väkevä, M., Koponen, I. K., Buzorius, G., and Kulmala, M.: Physical characterization of aerosol particles during nucleation events, Tellus B, 53(4), 344–358, doi:10.1034/j.1600-0889.2001.530403.x, 2001.

Baker, M. B. and Peter, T.: Small-scale cloud processes and climate, Nature, 451, 299–300, 2008.

Bennartz, R.: Global assessment of marine boundary layer cloud droplet number concentration from satellite, J. Geophys. Res., 112, D02201, doi:10.1029/2006JD007547, 2007.

Bennartz, R., Harshvardhan: Correction to "Global assessment of marine boundary layer cloud droplet number concentration from satellite", J. Geophys. Res., 112, D16302, doi:10.1029/2007JD008841, 2007.

Birmili, W., Berresheim, H., Plass-Dülmer, C., Elste, T., Gilge, S., Wiedensohler, A., and Uhrner, U.: The Hohenpeissenberg aerosol formation Experiment (HAFEX): a long-term study including size-resolved aerosol, H_2SO_4, OH, and monoterpenes measurements, Atmos. Chem. Phys., 3, 361–376, 2003,
http://www.atmos-chem-phys.net/3/361/2003/.

Aerosol formation in ECHAM5-HAM

R. Makkonen et al.

◄◄ | ►►

◄ | ►

Back | Close

Full Screen / Esc

Printer-friendly Version

Interactive Discussion

Camredon, M., Aumont, B., Lee-Taylor, J., and Madronich, S.: The SOA/VOC/NO$_x$ system: an explicit model of secondary organic aerosol formation, Atmos. Chem. Phys., 7, 5599–5610, 2007,
http://www.atmos-chem-phys.net/7/5599/2007/.

Chen, W.-T., Liao, H., and Seinfeld, J.: Future climate impacts of direct radiative forcing of anthropogenic aerosols, tropospheric ozone, J. Geophys. Res., 112, D14209, doi:10.1029/2006JD008051, 2007.

Chung, S. H. and Seinfeld, J. H.: Global distribution and climate forcing of carbonaceous aerosols, J. Geophys. Res., 107(D19), 4407, doi:10.1029/2001JD001397, 2002.

Engler, C., Rose, D., Wehner, B., Wiedensohler, A., Brüggemann, E., Gnauk, T., Spindler, G., Tuch, T., and Birmili, W.: Size distributions of non-volatile particle residuals (Dp<800 nm) at a rural site in Germany and relation to air mass origin, Atmos. Chem. Phys., 7, 5785–5802, 2007,
http://www.atmos-chem-phys.net/7/5785/2007/.

Forster, P., Ramaswamy, V., Artaxo, P., Berntsen, T., Betts, R., Fahey, D.W., Haywood, J., Lean, J., Lowe, D.C., Myhre, G., Nganga, J., Prinn, R., Raga, G., Schulz, M., and Van Dorland, R.: Changes in Atmospheric Constituents and in Radiative Forcing, in: Climate Change 2007: The Physical Science Basis. Contribution of Working Group I to the Fourth Assessment Report of the Intergovernmental Panel on Climate Change, edited by: Solomon, S., Qin, D., Manning, M., Chen, Z., Marquis, M., Averyt, K. B.,Tignor, M., and Miller, H. L., Cambridge University Press, Cambridge, United Kingdom and New York, NY, USA, 2007.

Fuzzi, S., Andreae, M. O., Huebert, B. J., Kulmala, M., Bond, T. C., Boy, M., Doherty, S. J., Guenther, A., Kanakidou, M., Kawamura, K., Kerminen, V.-M., Lohmann, U., Russell, L. M., and Pöschl, U.: Critical assessment of the current state of scientific knowledge, terminology, and research needs concerning the role of organic aerosols in the atmosphere, climate, and global scale, Atmos. Chem. Phys., 6, 2017–2038, 2006,
http://www.atmos-chem-phys.net/6/2017/2006/.

Gaydos, T. M., Stanier, C. O., and Pandis, S. N.: Modeling of in situ ultrafine atmospheric particle formation in the eastern United States, J. Geophys. Res., 110, D07S12, doi:10.1029/2004JD004683, 2005.

Ghan, S. J. and Schwartz, S. E.: Aerosol properties and processes: A path from field and laboratory measurements to global climate models, Bull. Amer. Meteor. Soc., 88, 1059–1083, 2007.

Aerosol formation in ECHAM5-HAM

R. Makkonen et al.

|◄ | ►|

◄ | ►

Back | Close

Full Screen / Esc

Printer-friendly Version

Interactive Discussion

Goto, D., Takemura, T., and Nakajima, T.: Importance of global aerosol modeling including secondary organic aerosol formed from monoterpene, J. Geophys. Res., 113, D07205, doi:10.1029/2007JD009019, 2008.

Griffin, R. J., Dabdub, D., and Seinfeld, J. H.: Development and initial evaluation of a dynamic species-resolved model for gas phase chemistry and size-resolved gas/particle partitioning associated with secondary organic aerosol formation, J. Geophys. Res., 110, D05304, doi:10.1029/2004JD005219, 2005.

Guillaume, B., Liousse, C., Rosset, R., Carchier, H., Van Velthoven, P., Bessagnet, B., and Poisson, N.: ORISAM-TM4: a new global sectional multi-component aerosol model including SOA formation – Focus on carbonaceous BC and OC aerosols, Tellus, 59B, 283–302, 2007.

Hoyle, C. R., Berntsen, T., Myhre, G., and Isaksen, I. S. A.: Secondary organic aerosol in the global aerosol – chemical transport model Oslo CTM2, Atmos. Chem. Phys., 7, 5675–5694, 2007,
http://www.atmos-chem-phys.net/7/5675/2007/.

Jones, A., Haywood, J. M., and Boucher, O.: Aerosol forcing, climate response and climate sensitivity in the Hadley Centre climate model, J. Geophys. Res., 112, D20211, doi:10.1029/2007JD008688, 2007.

Kanakidou, M., Seinfeld, J. H., Pandis, S. N., Barnes, I., Dentener, F. J., Facchini, M. C., Van Dingenen, R., Ervens, B., Nenes, A., Nielsen, C. J., Swietlicki, E., Putaud, J. P., Balkanski, Y., Fuzzi, S., Horth, J., Moortgat, G. K., Winterhalter, R., Myhre, C. E. L., Tsigaridis, K., Vignati, E., Stephanou, E. G., and Wilson, J.: Organic aerosol and global climate modeling: a review, Atmos. Chem. Phys., 5, 1053–1123, 2005,
http://www.atmos-chem-phys.net/5/1053/2005/.

Kazil, J., Lovejoy, E. R., Barth, M. C., and O'Brien, K.: Aerosol nucleation over oceans and the role of galatic cosmic rays, Atmos. Chem. Phys., 6, 4905–4924, 2006,
http://www.atmos-chem-phys.net/6/4905/2006/.

Kazil, J. and Lovejoy, E. R.: A semi-analytical method for calculating rates of new sulfate aerosol formation from gas phase, Atmos. Chem. Phys., 7, 3447–3459, 2007,
http://www.atmos-chem-phys.net/7/3447/2007/.

Kerminen, V.-M. and Kulmala, M.: Analytical formulae connecting the "real" and the "apparent" nucleation rate and the nuclei number concentration for atmospheric nucleation events, J. Aerosol Sci., 33, 609–622, 2002.

Kerminen, V.-M., Anttila, T., Lehtinen, K. E. J., and Kulmala, M.: Parameterization for atmo-

Aerosol formation in ECHAM5-HAM

R. Makkonen et al.

spheric new-particle formation: application to a system involving sulphuric acid and condensable water-soluble organic vapors, Aerosol Sci. Technol. 38, 1001–1008, 2004.

Kerminen, V.-M., Lihavainen, H., Komppula, M., Viisanen, Y., and Kulmala, M.: Direct observational evidence linking atmospheric aerosol formation and cloud droplet activation. Geophys. Res. Lett. 32, L14803, doi:10.1029/2005GL023130, 2005.

Komppula, M., Lihavainen, H., Hatakka, J., Paatero, J., Aalto, P., Kulmala, M., and Viisanen, Y.: Observations of new particle formation and size distributions at two different heights and surroundings in subarctic area in northern Finland, J. Geophys. Res., 108(D9), 4295, doi:10.1029/2002JD002939, 2003.

Koponen, I. K., Virkkula, A., Hillamo, R., Kerminen, V.-M., and Kulmala, M.: Number size distributions and concentrations of the continental summer aerosols in Queen Maud Land, Antarctica, J. Geophys. Res., 108(D18), 4587, doi:10.1029/2003JD003614, 2003.

Kuang, C. McMurry, P. H., McCormick, A. V., and Eisele, F.: Dependence of nucleation rates on sulphuric acid vapor concentrations in diverse atmospheric locations, J. Geophys. Res., 113, D10209, doi:10.1029/2007JD009253, 2008.

Kulmala, M., Pirjola, L., and Mäkelä, J. M.: Stable sulphate clusters as a source of new atmospheric particles, Nature 404, 66–69, 2000.

Kulmala, M., Vehkamäki, H., Petäjä, T., Dal Maso, M., Lauri, A., Kerminen, V.-M., Birmili, W., and McMurry, P. H.: Formation and growth rates of ultrafine atmospheric particles: A review of observations, J. Aerosol Sci. 35, 143–176, 2004a.

Kulmala, M., Kerminen, V.-M., Anttila, T., Laaksonen, A., and O'Dowd, C. D.: Organic aerosol formation via sulphate cluster activation, J. Geophys. Res. 109(D4), 4205, doi:10.1029/2003JD003961, 2004b.

Kulmala, M., Lehtinen, K. E. J., and Laaksonen, A.: Cluster activation theory as an explanation of the linear dependence between formation rate of 3nm particles and sulphuric acid concentration, Atmos. Chem. Phys., 6, 787–793, 2006,
http://www.atmos-chem-phys.net/6/787/2006/.

Kulmala, M., Riipinen, I., Sipilä, M., Manninen, H.E., Petäjä, T., Junninen, H., Dal Maso, M., Mordas, G., Mirme, A., Vana, M., Hirsikko, A., Laakso, L., Harrison, R. M., Hanson, I., Leung, C., Lehtinen, K. E. J., and Kerminen, V.-M.: Toward direct measurement of atmospheric nucleation, Science 318, 89–92. 10.1126/science.1144124, 2007b.

Laakso, L., Hussein, T., Aarnio, P., Komppula, M., Hiltunen, V., Viisanen, Y., and Kulmala, M.: Diurnal and annual characteristics of particle mass and number concentrations in urban, rural

and Arctic environments in Finland, Atmos. Environ., 37, 2629–2641, doi:10.1016/S1352-2310(03)00206-1, 2003.

Laaksonen, A. Hamed, A., Joutsensaari, J., Hiltunen, L., Cavalli, F., Junkermann, W., Asmi, A., Fuzzi, S., and Facchini, M. C.: Cloud condensation nucleus production from nucleation events at a highly polluted region, Geophys. Res. Lett. 32, L06812, doi:10.1029/2004GL022092, 2005.

Lack, D. A., Tie, X. X., Bofinger, N. D., Wiegand, A. N., and Madronich, S.: Seasonal variability of secondary organic aerosol: A global modeling study, J. Geophys. Res., 109, D03203, doi:10.1029/2003JD003418, 2004.

Lehtinen, K. E. J., Dal Maso, M., Kulmala, M., and Kerminen, V.-M.: Estimating nucleation rates from apparent particle formation rates and vice versa: Revised formulation of the Kerminen-Kulmala equation, J. Aerosol Sci., 38, 988–994, 2007.

Lihavainen, H., Kerminen, V.-M., Komppula, M., Hatakka, J., Aaltonen, V., Kulmala, M., and Viisanen Y.: Production of "potential" cloud condensation nuclei associated with atmospheric newparticle formation in northern Finland. J. Geophys. Res. 108(D24), 4782, doi:10.1029/2003JD003887, 2003.

Lohmann, U. and Feichter, J.: Global indirect aerosol effects: a review, Atmos. Chem. Phys., 5, 715–737, 2005,
http://www.atmos-chem-phys.net/5/715/2005/.

Lohmann, U., Stier, P., Hoose, C., Ferrachat, S., Kloster, S., Roeckner, E., and Zhang, J., Cloud microphysics and aerosol indirect effects in the global climate model ECHAM5-HAM, Atmos. Chem. Phys., 7, 3425–3446, 2007,
http://www.atmos-chem-phys.net/7/3425/2007/.

Lucas, D. D. and Arimoto, H.: Evaluating aerosol nucleation parameterizations in a global atmospheric model, Geophys. Res. Lett. 33, L10808, doi:10.1029/2006GL025672, 2006.

McMurry, P. H., Fink, M., Sakurai, H., Stolzenburg, M. R., Mauldin, R. L., Smith, J, Eisele, F., Moore, K., Sjostedt, S., Tanner, D., Huey, L. G., Nowak, J. B., Edgerton, E., and Voisin, D.: A criterion for new particle formation in the sulfur-rich Atlanta atmosphere, J. Geophys. Res., 110, D22S02, doi:10.1029/2005JD005901, 2005.

Merikanto, J., Napari, I., Vehkamäki, H., Anttila, T., and Kulmala, M.: New parameterization of sulphuric acid-ammonia-water ternary nucleation rates at tropospheric conditions, J. Geophys. Res., 11, D15207, doi:10.1029/2006JD007977, 2007.

Miles, N. L., Verlinde, J., and Clothiaux, E. E.: Cloud droplet size distributions in low-level

stratiform clouds, J. Atmos. Sci. 57, 295–311, 2000.

Modgil, M. S., Kumar S., Tripathi, S. N., and Lovejoy, E. R.: A parameterization of ion-induced nucleation of sulphuric acid and water for atmospheric conditions, J. Geophys. Res., 110, D19205, doi:10.1029/2004JD005475, 2005.

5 Napari, I., Noppel, M., Vehkamäki, H., and Kulmala, M.: Parameterization of ternary nucleation rates for H_2SO_4-NH_3-H_2O vapors, J. Geophys. Res., 107(D19), 4381, doi:10.1029/2002JD002132, 2002.

O'Dowd, C. D., Geever, M., Hill, M. K., Smith, M. H., and Jennings S. G.: New Particle Formation: Nucleation Rates and Spatial Scales in the Clean Marine Coastal Environment,
10 Geophys. Res. Lett., 25(10), 1661–1664, 1998.

Penner, J. E., Quaas, J., Storelvmo, t., Takemura, T., Boucher, O., Guo, H., Kirkevåg, A., Kristjansson, J. E., and Seland, Ø: Model intercomparison of indirect aerosol effects, Atmos. Chem. Phys., 6, 3391–3405, 2006,
http://www.atmos-chem-phys.net/6/3391/2006/.

15 Pierce, J. R., Chen, K., and Adams, P. J.: Contribution of primary carbonaceous aerosol to cloud condensation nuclei: processes and uncertainties evaluated with a global aerosol microphysics model, Atmos. Chem. Phys., 7, 5447–5466, 2007,
http://www.atmos-chem-phys.net/7/5447/2007/.

Pun, B. K. and Seigneur, C.: Investigative modeling of new pathways for secondary organic
20 aerosol formation, Atmos. Chem. Phys., 7, 2199–2216, 2007,
http://www.atmos-chem-phys.net/7/2199/2007/.

Riipinen, I., Sihto, S.-L., Kulmala, M., Arnold, F., Dal Maso, M., Birmili, W., Saarnio, K., Teinilä, K., Kerminen, V.-M., Laaksonen, A., and Lehtinen, K. E. J.: Connections between atmospheric sulphuric acid and new particle formation during QUEST III - IV campaigns in
25 Hyytiälä and Heidelberg, Atmos. Chem. Phys. 7, 1899–1914, 2007.

Rissler, J., Vestin, A., Swietlicki, E., Fisch, G., Zhou, J., Artaxo, P., and Andreae, M. O.: Size distribution and hygroscopic properties of aerosol particles from dry-season biomass burning in Amazonia, Atmos. Chem. Phys., 6, 471–491, 2006,
http://www.atmos-chem-phys.net/6/471/2006/.

30 Shindell, D. T., Faluvegi, G., Bauer, S. E., Koch, D., Unger, N., Menon, S., Miller R. L., Schmidt, G. A., and Streets, D. G.: Climate response to projected changes in short-lived species under an A1B scenario from 2000–2050 in the GISS climate model, J. Geophys. Res., 112, D20103, doi:10.1029/2007JD008753, 2007.

Title Page

Abstract | Introduction

Conclusions | References

Tables | Figures

|◄ | ►|

◄ | ►

Back | Close

Full Screen / Esc

Printer-friendly Version

Interactive Discussion

Sihto, S.-L., Kulmala, M., Kerminen, V.-M., Dal Maso, M., Petäjä, T., Riipinen, I., Korhonen, H., Arnold, F., Janson, R., Boy, M., Laaksonen, A., and Lehtinen, K. E. J.: Atmospheric sulfuric acid and aerosol formation: implications from atmospheric measurements for nucleation and early growth mechanisms, Atmos. Chem. Phys. 6, 4079–4091, 2006.

Spracklen, D. V., Carslaw, K. S., Kulmala, M., Kerminen, V.-M., Mann, G. W., and Sihto, S.-L.: The contribution of boundary layer nucleation events to total particle concentrations on regional and global scales, Atmos. Chem. Phys., 6, 5631–5648, 2006,
http://www.atmos-chem-phys.net/6/5631/2006/.

Spracklen, D. V., Carslaw, K. S., Kulmala, M., Kerminen, V.-M., Sihto, S.-L., Riipinen, I., Merikanto, J., Mann, G. W., Chipperfield, M. P., Wiedensohler, A., Birmili, W., and Lihavainen H.: Contribution of particle formation to global cloud condensation nuclei concentrations, Geophys. Res. Lett., 35, L06808, doi:10.1029/2007GL033038, 2008.

Ström, J., Umegård, J., Tørseth, K., Tunved, P., Hansson, H.-C., Holmén, K., Wismann, V., Herber, A., and König-Langlo, G.: One year of particle size distribution and aerosol chemical composition measurements at the Zeppelin Station, Svalbard, March 2000–March 2001, Phys. Chem. Earth, 28, 1181–1190, 2003.

Suni, T., Kulmala, M., Hirsikko, A., Bergman, T., Laakso, L., Aalto, P. P., Leuning, R., Cleugh, H., Zegelin, S., Hughes, D., van Gorsel, E., Kitchen, M., Vana, M., Hrrak, U., Mirme, S., Mirme, A., Sevanto, S., Twining, J., and Tadros, C.: Formation and characteristics of ions and charged aerosol particles in a native Australian Eucalypt forest, Atmos. Chem. Phys., 8, 129–139, 2008,
http://www.atmos-chem-phys.net/8/129/2008/.

Textor, C., Schulz, M., Guibert, S., Kinne, S., Balkanski, Y., Bauer, S., Berntsen, T., Berglen, T., Boucher, O., Chin, M., Dentener, F., Diehl, T., Feichter, J., Fillmore, D., Ginoux, P., Gong, S., Grini, A., Hendricks, J., Horowitz, L., Huang, P., Isaksen, I. S. A., Iversen, T., Kloster, S., Koch, D., Kirkevåg, A., Kristjansson, J. E., Krol, M., Lauer, A., Lamarque, J. F., Liu, X., Montanaro, V., Myhre, G., Penner, J. E., Pitari, G., Reddy, M. S., Seland, Ø., Stier, P., Takemura, T., and Tie, X.: The effect of harmonized emissions on aerosol properties in global models – an AeroCom experiment, Atmos. Chem. Phys., 7, 4489–4501, 2007,
http://www.atmos-chem-phys.net/7/4489/2007/.

Tulet, P., Grini, A., Grifin, R., J., and Peticol, S.: ORILAM-SOA: A computationally efficient model for predicting secondary organic aerosols in three-dimensional atmospheric models, J. Geophys. Res., 111, D23208, doi:10.1029/2006JD007152, 2006.

Title Page

Abstract | Introduction

Conclusions | References

Tables | Figures

|◄ | ►|

◄ | ►

Back | Close

Full Screen / Esc

Printer-friendly Version

Interactive Discussion

Tsigaridis, K. and Kanakidou, M.: Global modelling of secondary organic aerosol in the tropo-sphere: a sensitivity analysis, Atmos. Chem. Phys., l3, 1849–1869, 2003.

Vehkamäki, H., Kulmala, M., Napari, I., Lehtinen, K. E. J., Timmreck, C., Noppel, M., and Laaksonen, A.: An improved parameterization for sulphuric acid-water nucleation rates for tropospheric and stratospheric conditions, J. Geophys. Res., 107(D22), 4622, doi:10.1029/2002JD2184, 2002.

Volkamer, R., Jimenez, J. L., San Martini, F., Dzepina, K, Zhang, Q., Salcedo, D., Molina, L. T., Worsnop, D. R., and Molina, M. J.: Sencondary organic aerosol formation from anthro-pogenic air pollution: Rapid and higher than expected, Geophys. Res. Lett., 33, L17811, doi:10.1029/2006GL026899, 2006.

Aerosol formation in ECHAM5-HAM

R. Makkonen et al.

Table 1. Experiment names, nucleation methods and BSOA method of different experiments. Experiment B is a reference simulation, since it is simulated with standard ECHAM5-HAM.

Experiment	Nucleation method	BSOA method
B	Binary	Standard ECHAM5-HAM
A0	Activation ($A=2\times10^{-7}\,s^{-1}$) and Binary	Standard ECHAM5-HAM
A1	Activation ($A=2\times10^{-6}\,s^{-1}$) and Binary	Standard ECHAM5-HAM
A2	Activation ($A=2\times10^{-5}\,s^{-1}$) and Binary	Standard ECHAM5-HAM
AS1	Activation ($A=2\times10^{-6}\,s^{-1}$) and Binary	Condensing BSOA (Yield 0.07)
AS2	Activation ($A=2\times10^{-6}\,s^{-1}$) and Binary	Condensing BSOA (Yield 0.15)
S0	Binary	Condensing BSOA (Yield 0.025)
S1	Binary	Condensing BSOA (Yield 0.07)
S2	Binary	Condensing BSOA (Yield 0.15)

Table 2. Annual median number concentrations [cm^{-3}] of aerosol sizes D_p>10 nm and D_p>100 nm from observations and different experiments. On each row, closest model value to observation is emphasized. Observational data is taken from CREATE aerosol database (http://www.nilu.no/projects/ccc/create/database.htm), except for Himalaya.

D_p>10 nm	Observation	B	A0	A1	A2	AS1	AS2	S0	S1	S2
Hyytiälä	1277[a]	713	**1269**	1590	1651	2161	2097	519	666	482
Melpitz	4405[b]	1908	**4161**	5307	6577	6415	6667	1983	1839	1808
Hohenheissenberg	2362[c]	**2019**	2773	3505	3676	4087	4313	1813	1747	1882
Zeppelin	133[d]	**126**	342	417	454	405	401	113	117	118
Mace Head	553[e]	298	**701**	1086	1174	1004	1033	264	298	291
Himalaya	2008[f]	**1932**	6216	8776	8904	9198	9529	1592	1640	1633
Pallas	267[g]	398	749	984	867	1447	1453	**343**	434	351
D_p>100 nm										
Hyytiälä	489[a]	388	**454**	405	379	258	310	189	247	210
Melpitz	1557[b]	1001	1074	1045	**1135**	1037	1130	1040	917	932
Hohenheissenberg	718[c]	1299	1297	1320	1287	1165	1325	1148	**1082**	1211
Zeppelin	61[d]	22	31	**34**	**34**	27	24	18	22	19
Mace Head	135[e]	53	84	**120**	112	105	115	50	60	62
Himalaya	926[f]	1225	1429	1523	1832	1384	1349	**1060**	1072	1065
Pallas	104[g]	151	162	163	160	73	**88**	42	62	51

[a] Aalto et al., 2001, data from year 2000.
[b] Engler et al., 2007, data from year 2003.
[c] Birmili et al., 2003, data from year 2000.
[d] Ström et al., 2003, data from year 2003.
[e] O'Dowd et al., 1998, data from year 2003.
[f] Komppula et al., 2008*, data from year 2006.
[g] Komppula et al., 2003, data from year 2001.
* Komppula M., Lihavainen, H., Hyvärinen, A.-P., Kerminen, V.-M., Panwar, T. S., Sharma, V. P., and Viisanen, Y.: Physical properties of aerosol particles at a Himalayan background site in India, submitted to J. Geophys. Res., 2008.

Title Page

Abstract | Introduction

Conclusions | References

Tables | Figures

|◄ | ►|

◄ | ►

Back | Close

Full Screen / Esc

Printer-friendly Version

Interactive Discussion

Table 3. Annual average CDNC [cm^{-3}] in selected areas (as seen in Fig. 12) in different experiments. The reference values are from Bennartz et al. (2006) and are results of two and a half year averages of satellite observations. The simulated values which are within the error estimates of reference values are shown in bold letters.

Experiment	SAF	SAM	NAM	NEA	NAF
B	47	34	52	49	47
A0	**88**	**79**	**99**	89	**108**
A1	121	114	154	**135**	179
A2	155	155	176	**151**	224
AS1	123	120	155	**133**	188
AS2	118	120	143	**136**	173
S0	49	36	50	49	46
S1	46	37	53	45	45
S2	48	36	49	43	44
Reference value	95±23	77±36	96±26	129±23	95±23
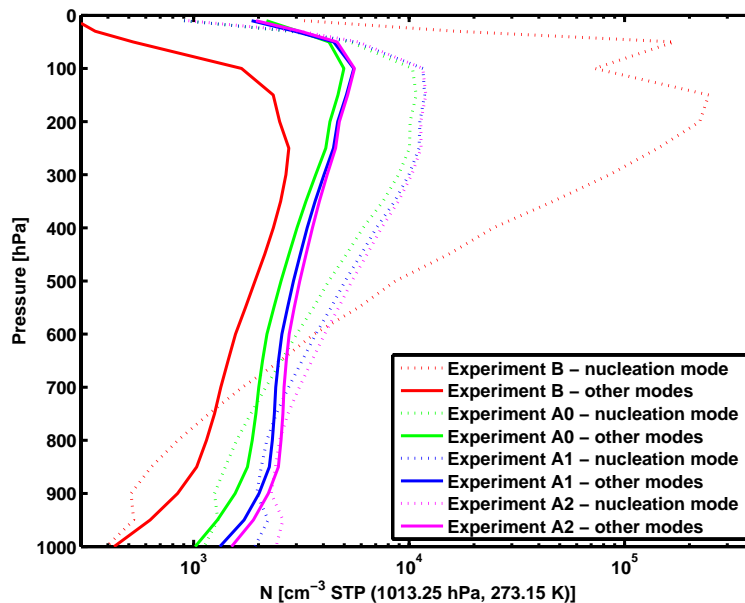
Fig. 1. Annual global averages of aerosol number concentrations as a function of altitude. Dotted line represents nucleation mode concentration and solid line the total number concentration neglecting nucleation mode.
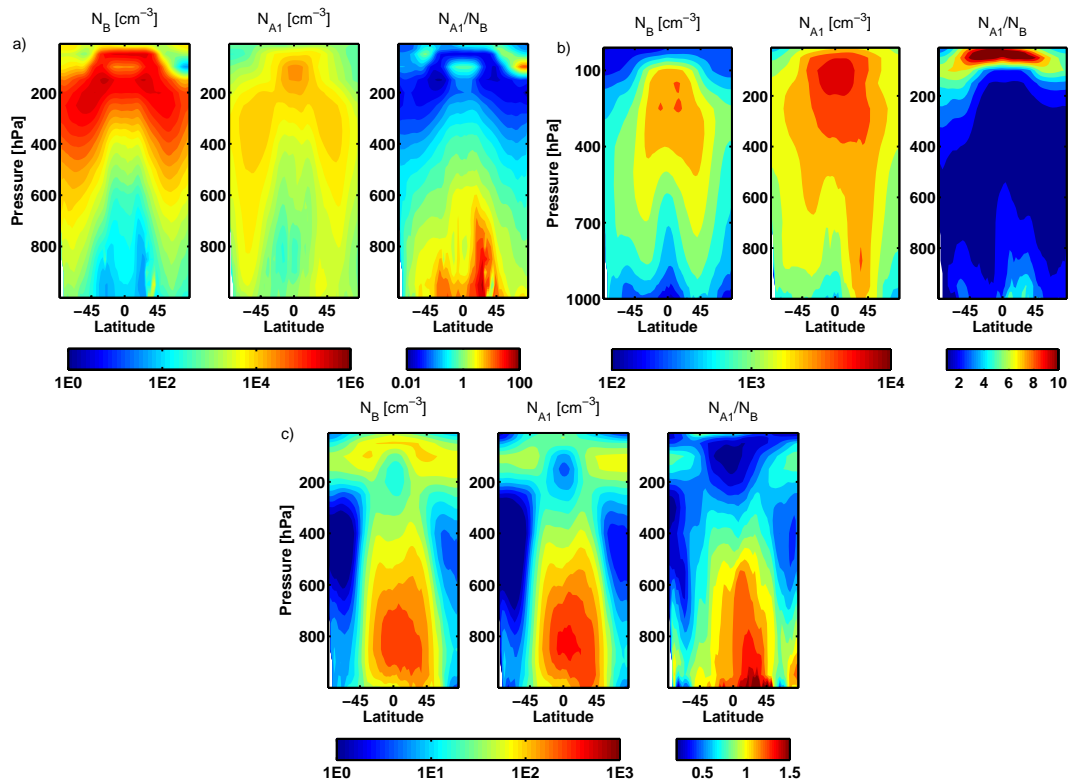
Fig. 2. Annual zonal average concentrations [cm^{-3} STP (1013.25 hPa, 273.15 K)] of **(a)** nucleation mode aerosol number; **(b)** sum of Aitken mode number concentration; and **(c)** sum of accumulation mode number concentration. Left panels show the Experiment B (standard ECHAM-HAM); centre ones Experiment A1 (using activation nucleation in addition to the standard binary nucleation); and right panels show the ratio of the yearly averages for Experiments B and A1. Notice the different color scales between figures.

Full Screen / Esc

Printer-friendly Version

Interactive Discussion
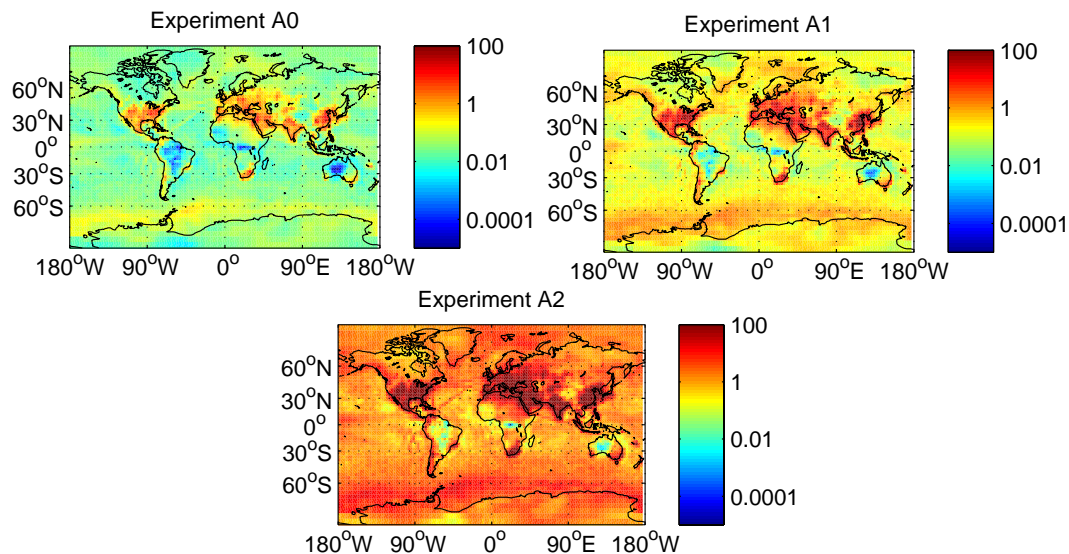
Fig. 3. Annual average nucleation rates [cm^{-3} s^{-1}] in the surface layer using different values for activation coefficient *A*.
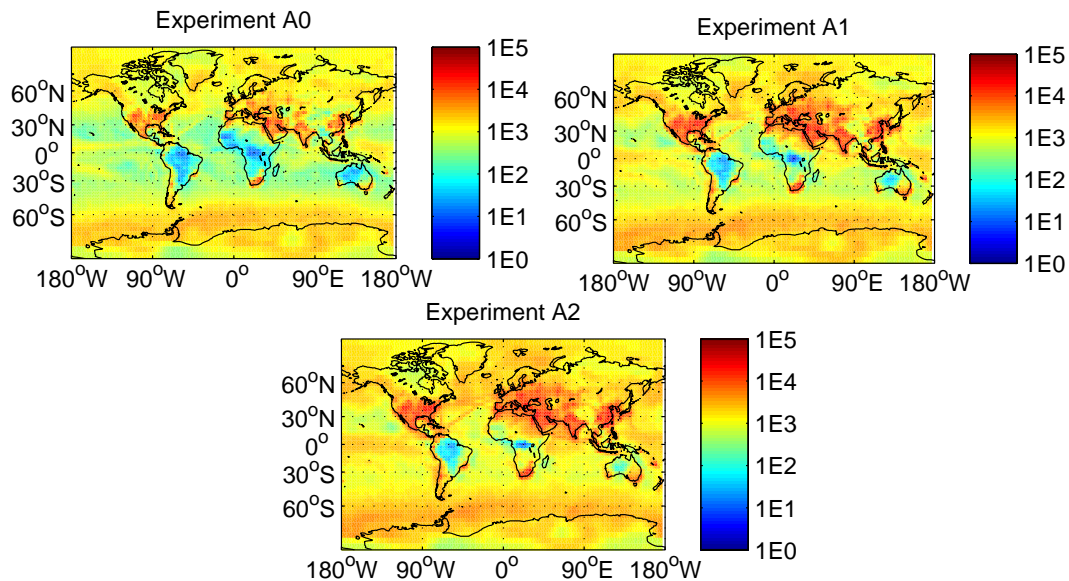
Fig. 4. Annual average nucleation mode number concentration [cm^{-3}] in the surface layer.
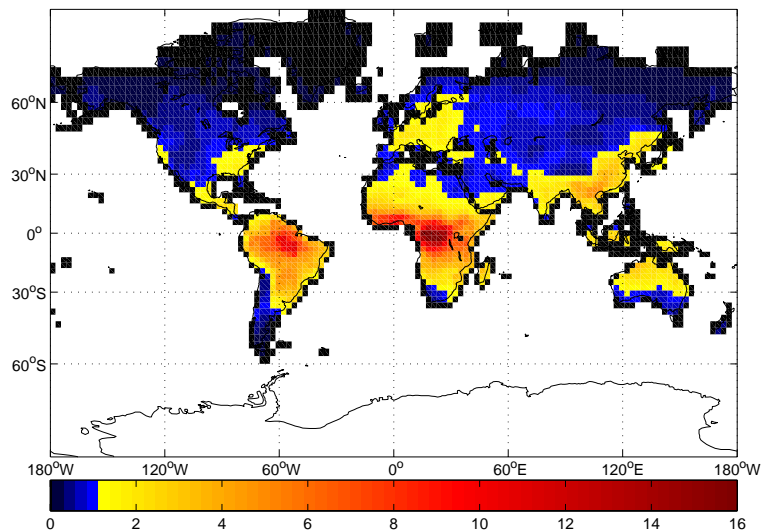
Fig. 5. Ratio (flux to soluble accumulation mode)/(flux to soluble Aitken mode) for biogenic organics using dynamic BSOA formation mechanism (Experiment AS2). Standard ECHAM5-HAM assumes a 1:1 ratio.
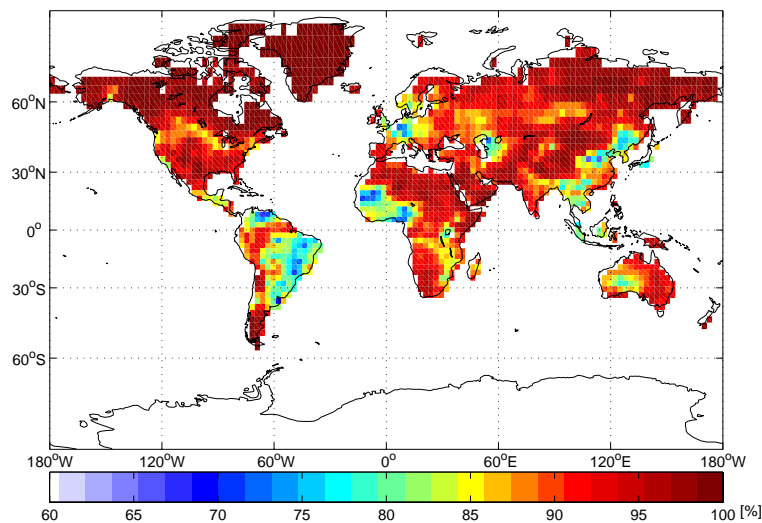
Fig. 6. Fraction of biogenic organics condensing to soluble modes in Experiment AS2. In standard ECHAM5-HAM, a constant fraction of 65% is assumed, however, in Experiment AS2, grid box average is always above 65%.
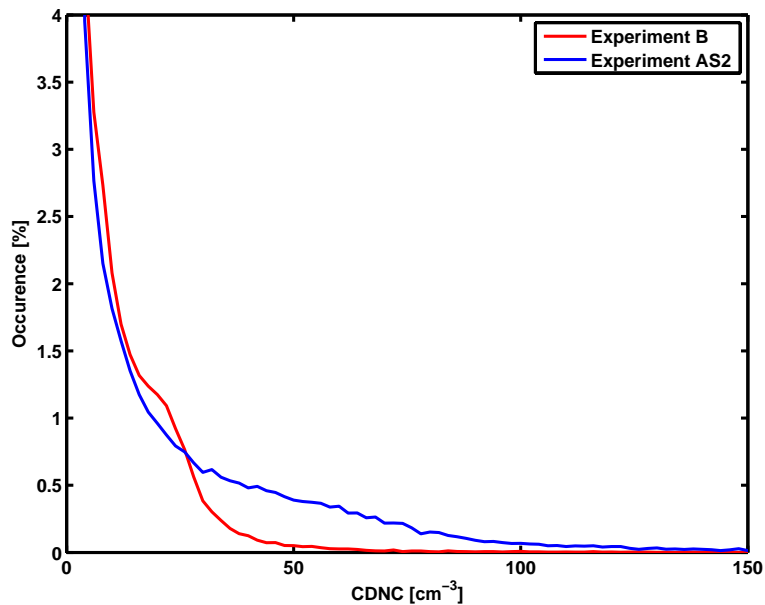
Fig. 7. Distribution of CDNC in annual average cloud-field in Experiments B and AS2.
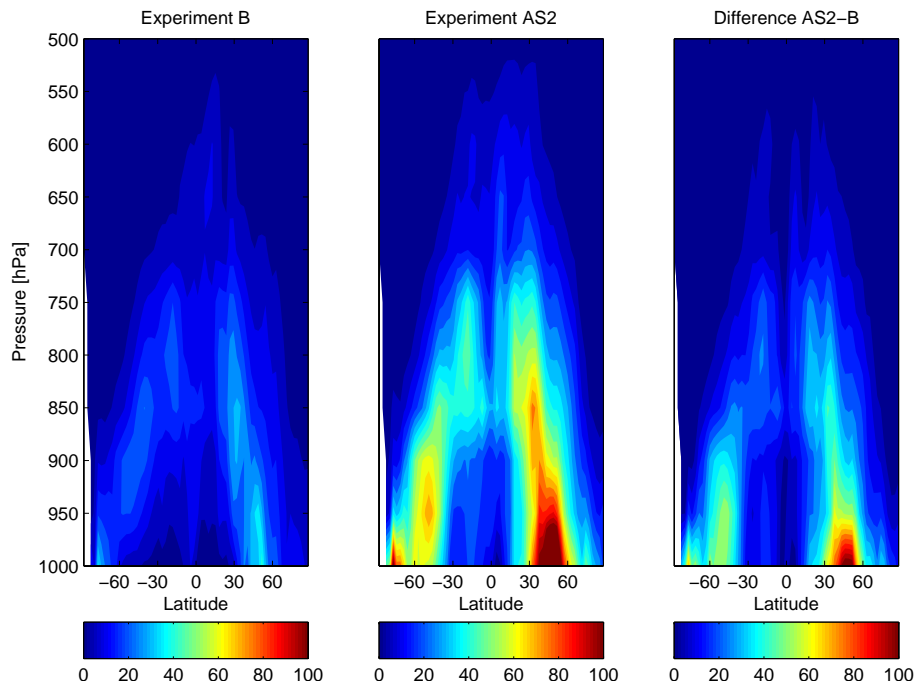
Fig. 8. Annual zonal average CDNC [cm^{-3}] in Experiments B and AS2 and their difference.

Full Screen / Esc

Printer-friendly Version

Interactive Discussion
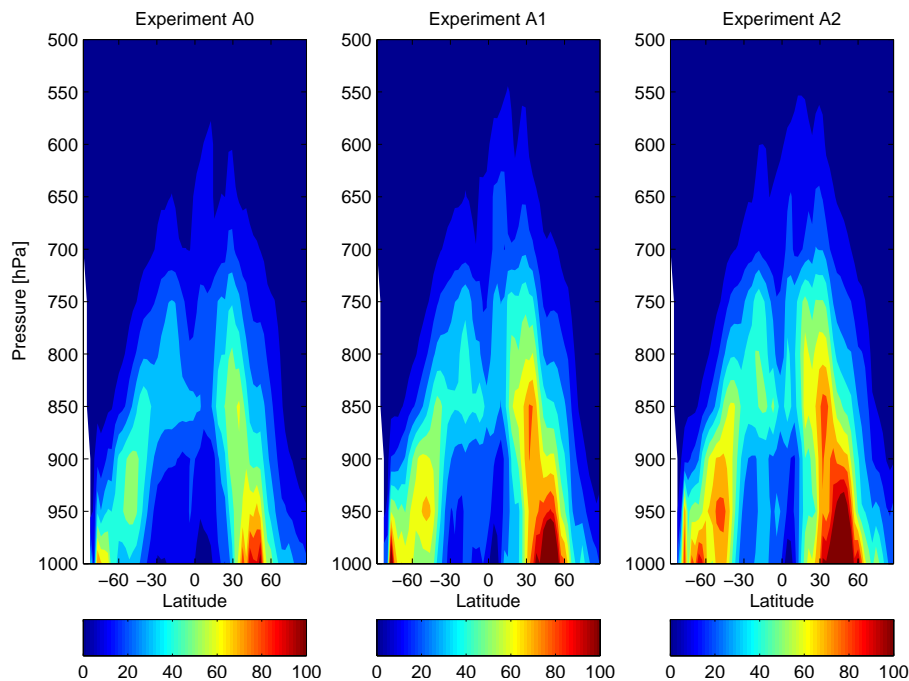
Fig. 9. Sensitivity of annual zonal average CDNC [cm^{-3}] to the activation coefficient A.
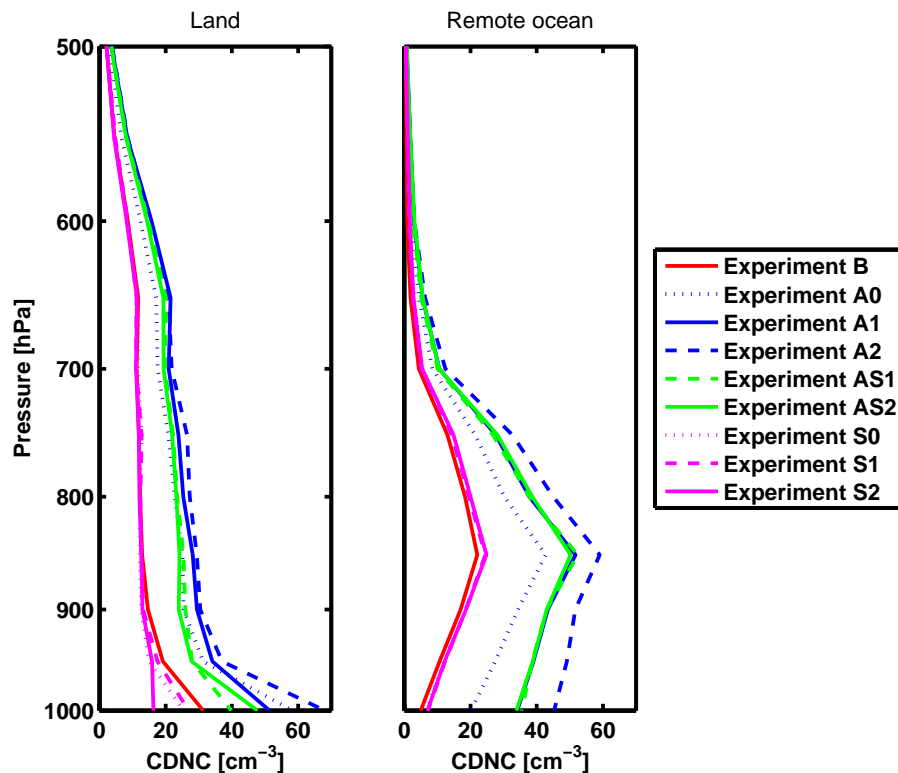
Fig. 10. Annual vertical average CDNC above land and remote oceans. Experiment B is in red; Experiments with activation-type nucleation (A0, A1, A2) in blue; Experiments with dynamic BSOA condensation, but only binary nucleation in magenta (S0, S1, S2); Experiments with activation-type nucleation and dynamic BSOA condensation in green (AS1, AS2).
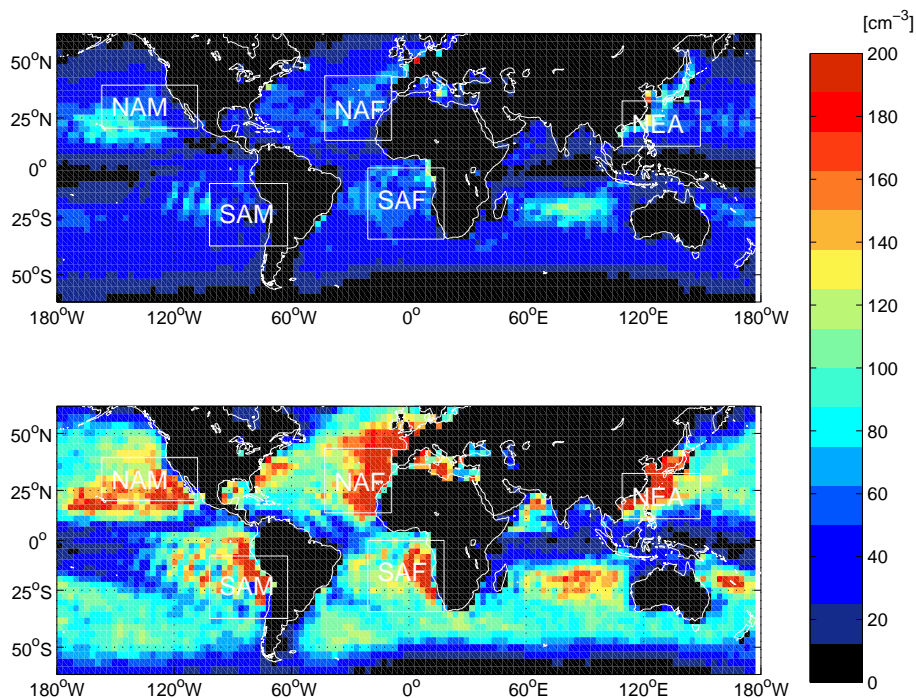
Fig. 11. Annual average cloud-top CDNC in Experiments B (top) and AS2 (below). The scales and specific areas (NAM, SAM, NAF, SAF and NEA) are chosen to match Fig. 5 of Bennartz et al. (2006) for satellite measurements over 2.5 year period. The concentrations are only shown over oceans for easy comparison with satellite data.